

Non-crystalline structures in the growth of silver nanoclusters

 F. Baletto¹, C. Mottet², and R. Ferrando^{1,a}
¹ INFM and CFSBT/CNR, Dipartimento di Fisica dell'Università di Genova, via Dodecaneso 33, 16146 Genova, Italy

² CRMC2/CNRS, Campus de Luminy, Case 913, 13288 Marseille Cedex 9, France

Received 28 November 2000

Abstract. The growth of nanometer-size free Ag clusters is studied by Molecular Dynamics simulations. The morphology transition from the icosahedron at the magic size of $N = 55$ atoms to the Marks truncated decahedron at $N = 75$ is analyzed in details, in order to single out kinetic trapping and entropic effects. At very low T , the cluster is kinetically trapped in an icosahedral structure. At intermediate T the transition takes place sharply at $N \simeq 65$. At higher T , the transition is smeared out and finally, around 550 K no transition is found because the 75 decahedron is melted.

PACS. 61.46.+w Nanoscale materials: clusters, nanoparticles, nanotubes, and nanocrystals

1 Introduction

The study of the structure of free nanoclusters is a basic step for understanding their physical and chemical properties, mostly related to catalysis and surface nanostructuring [1–3]. Recently, several studies focused on the energetics of noble and transition metal clusters [4–8], showing that at small sizes ($N < 100$ atoms) clusters prefer in most cases non-crystalline structures as minimum-energy structures. For example, for Ag clusters, both Sutton-Chen [7] and tight-binding [8, 9] potentials predict that at the magic number $N = 55$ the Mackay icosahedron (Ih) [10] is the most favourable structure, and at $N = 75$ the (2, 2, 2) Marks truncated decahedron (m -Dh) [10, 11] is the best structure. At $N = 38$, the most stable structure is a truncated octahedron (TO) [7, 8]. In Ref. [7], the complete sequence of minimum-energy structures of Ag clusters as a function of the size N has been calculated by Sutton-Chen potentials. There, at $55 \leq N \leq 75$, it has been found that Ih structures are favourable up to $N = 62$, and Dh structures for larger sizes. From these results one could trace a minimum-energy “growth sequence” for Ag clusters. However, the minimum-energy growth sequence is not always followed in typical experimental conditions [12]. In fact, it has been shown by Molecular Dynamics (MD) simulations [9] that long-lived metastable structures can be grown at sizes above $N = 100$ in a wide range of growth conditions (temperature T and deposition flux $\phi = \tau^{-1}$, where τ is the deposition time interval). These metastable structures are formed because of a kinetic trapping phenomenon, which takes place when growth is too fast to let the cluster optimize its free energy at the given T . Moreover, even if the cluster is able to optimize its free

energy on the growth time scale, it is not always true that the minimum-energy structure is also the minimum-free-energy structure, especially if T is high. Because of that, a study of the growth of clusters [9, 13, 14] is important, and gives much information beyond the total-energy minimization. In this paper we study the growth of Ag clusters by MD simulations. We consider sizes up to $N = 100$, focusing on sizes $55 \leq N \leq 75$. In Section 2 we give a brief account of our model and methods. Section 3 contains the results and Section 4 is devoted to the conclusions.

2 Model and methods

Silver is modeled by tight-binding many-body potentials as developed within the second-moment approximation to the tight-binding model [15]. The form and the parameters of the potentials are given in Ref. [14]. In our growth simulations, we deposit atoms one by one with a time interval $\tau = \phi^{-1}$, starting from a seed of 7 atoms. In the following, we fix $\tau = 7$ ns, if not otherwise specified. This deposition time is of the order of those in growth experiments [12] in Inert Gas Aggregation sources (for a discussion see [9]). We keep the cluster at constant T by an Andersen thermostat, whose collision frequency is chosen in order to insure efficient thermalization without altering the diffusive properties of the atoms in the cluster [14]. The cluster structure during growth is monitored by the Common Neighbor Analysis (CNA) [16]. We assign to each couple of nearest-neighbor (NN) atoms a CNA signature. This signature is a triplet of integers (r, s, t) (do not confuse this triplet with the triplet describing the truncation in the m -Dh structures [11]). r is the number of common nearest neighbors of two atoms of the couple, s is the number of nearest-neighbor bonds among

^a e-mail: ferrando@fisica.unige.it

Table 1. CNA for perfect structures at magic numbers.

N	Structure	$P(5, 5, 5)$	$P(4, 2, 1)$	$P(4, 2, 2)$
55	TO	0.00	55.6	0.00
55	Ih	10.3	0.00	38.5
55	(3, 3, 1) m -Dh	1.83	22.8	29.7
75	(2, 2, 2) m -Dh	1.25	28.2	20.4
79	TO	0.00	50.0	0.00

the r common nearest neighbors, and t is the length of the longest chain which can be formed with the s bonds [16]. We have found that the monitoring of the signatures $(r, s, t) = (5, 5, 5)$, $(4, 2, 1)$, $(4, 2, 2)$ is sufficient to distinguish icosahedral, decahedral and fcc structures in the size range of our simulations. In Table 1 we report the percentages $P(5, 5, 5)$, $P(4, 2, 1)$ and $P(4, 2, 2)$ of the above signatures over the total number of signatures in the cluster (*i.e.* the ratio between the couples with a given signature to the total number of nearest-neighbor couples in the cluster), for some perfect structures at magic numbers, and specifically the 55 and 79 TO (the former being a cuboctahedron), the 55 Ih and for the 75 (2, 2, 2) m -Dh. In particular, $P(5, 5, 5)$ is important to identify local fivefold symmetries. In fact, the couples of nearest-neighbor atoms which are located along a (locally) fivefold axis, have the $(5, 5, 5)$ signature. Therefore $P(5, 5, 5)$ is much larger in Ih than in Dh of comparable size and it is zero in fcc clusters. On the other hand, $P(4, 2, 1)$ is large (close to 50%) for fcc clusters, intermediate for Dh and small for Ih (indeed, it is zero for the 55 Ih), while for $P(4, 2, 2)$ the opposite happens. In our growth simulations we have monitored the CNA signatures by averaging over at least 100 snapshots at each size N .

3 Results

As written in the Introduction, we focus on the growth in the interval $55 \leq N \leq 75$ atoms, whose extrema are magic numbers for Ih and Dh structures respectively. At these small sizes, the growing cluster is able to optimize its structure on the time scale in between subsequent depositions already at rather low T . This gives a wide window where T is high enough to avoid kinetic trapping effects (see the following discussion) and, on the other hand, where T is sufficiently low to allow the growth of well-ordered (non-melted) structures around the magic numbers. We shall see that, at the deposition time $\tau = 7$ ns, this window is roughly $350 \leq T \leq 500$ K. We remark that at larger sizes ($N \simeq 150$), kinetic trapping effects, leading to the growth of well-ordered metastable structures, are important up to quite high T [9], like 550 K, so that kinetic effects on the morphology transitions are not easily avoided. On the contrary, at small sizes, the growth simulations allow to study the effect of temperature on the transition from structures of Ih symmetry to structures of Dh symmetry without important kinetic effects.

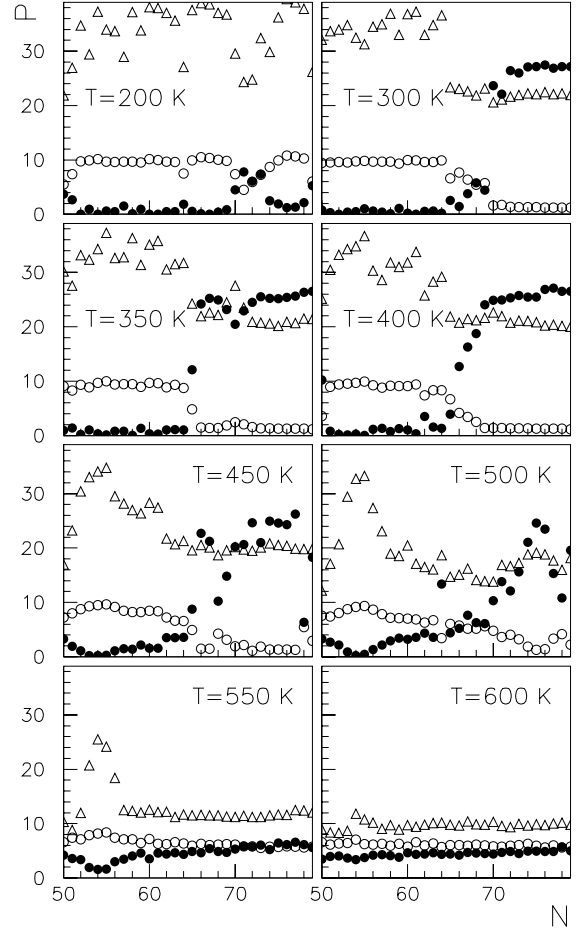


Fig. 1. CNA at different temperatures. $P(5, 5, 5)$, $P(4, 2, 1)$ and $P(4, 2, 2)$ are reported as a function of N and they are represented by open circles, full circles and open triangles respectively. The transition Ih \rightarrow Dh is completed when both $P(5, 5, 5)$ decreases to ~ 1 –2% and $P(4, 2, 1)$ becomes larger than $P(4, 2, 2)$. This transition is seen in the range $300 \leq T \leq 500$ K.

Our results are summarized by Figs. 1-4. In Fig. 1 we report the CNA analysis of typical simulations at several different temperatures in the range 200–600 K, and in Fig. 2 we report the average parameter $\overline{\Delta}(N) = [\overline{E}(N) - \varepsilon_B N]/N^{2/3}$, where $\overline{E}(N)$ is the average total energy at a given size (and temperature), and ε_B is the cohesive energy per atom, as a function of the size again at different temperatures. In Figs. 3 and 4, we present snapshots from two typical simulations at different temperatures (350 and 500 K). From these results we try at first to determine the temperature above which kinetic trapping effects are no more important. If we look at the results at $T = 200$ K (see Fig. 1), we see that the growing cluster retains its icosahedral symmetry up to $N = 75$: $P(5, 5, 5)$ stays practically constant at about 10%, $P(4, 2, 1)$ is always close to zero, and $P(4, 2, 2)$ is the highest one. These signatures characterize the icosahedral symmetry (see Table 1). Icosahedra are perfect at $N = 55$, and defected (with an incomplete shell) at larger

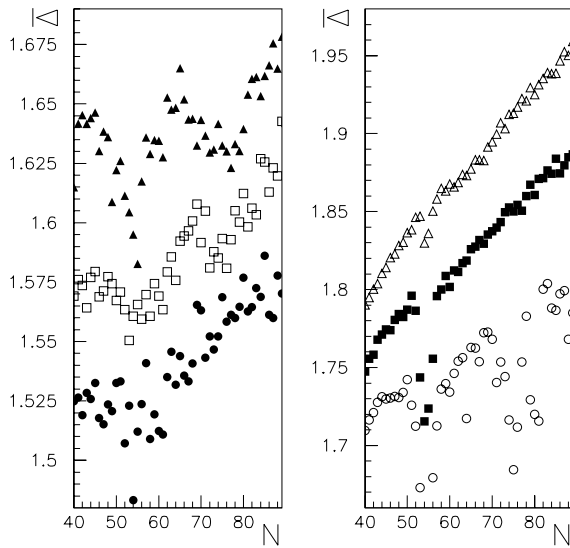


Fig. 2. Average parameter $\bar{\Delta}(N)$ at six different temperatures. Left panel: $T = 200$ K (full circles), $T = 300$ K (open squares), and $T = 400$ K (full triangles). Right panel: $T = 500$ K (open circles), $T = 550$ K (full squares), and $T = 600$ K (open triangles).

sizes. The almost perfect Ih structures give a minimum in $\bar{\Delta}(N)$ around $N = 55$, as seen in Fig. 2. Since we know that at $N = 75$ the $(2, 2, 2)m$ -Dh is the best structure [7–9], the persistence of the Ih symmetry is a clear indication of kinetic trapping. At such low T it is unlikely that the entropic contribution would change what is found from the total-energy minimization, thus giving that Ih structures are more stable than Dh ones at $N = 75$. If this would be the case, at higher T we should find again Ih clusters at that size. However, this is not the case: growing at 300 K, a clear transition from Ih to Dh structures is seen above $N = 65$. This transition is characterized by a drop of $P(5, 5, 5)$ and of $P(4, 2, 2)$ and by a rise of $P(4, 2, 1)$. Thus, at 300 K kinetic trapping effects are mostly overcome, even if not completely, as can be seen in the results of Fig. 1. In fact, at 300 K the transition is not sharp, and there is an interval $65 \leq N \leq 69$ where structures are hybrid, not easily classified neither as Ih nor as Dh. At $N \geq 70$ clusters grow clearly as decahedra, even if with some defects. At 350 K, the transition is sharper, and takes place at $N = 65$ –66. At $N = 75$ it is likely to find almost perfect $(2, 2, 2)m$ -Dh, with no defects or with a few of them. This gives a minimum in $\bar{\Delta}(N)$ also at $N = 75$. In the range 350–450 K the transition to clear Dh structures takes place at the lowest size compared to any other T considered here. This indicates that, starting from 350 K, kinetic trapping effects are no more important, and the growing cluster is able to optimize its free energy on the time scale of the simulations. Snapshots from a simulation at 350 K are given in the first and second columns of Figs. 3 and 4; especially from the snapshots in the second column, the transition from Ih structures (the ones in the first five snapshots of Fig. 3, taken at $N = 55, 57, 59, 61, 63$) to Dh structures (the last snapshot

in Fig. 3, taken at $N = 65$, and all the following snapshots in Fig. 4) can be clearly seen. The results at 400 K and at 450 K are not so different from those at 350 K; at these temperatures we have the largest size range where Dh structures are grown below $N = 75$. The only difference between 350 K and 400–450 K is that one can spot a tendency of the transition to become less sharp with increasing temperature. This tendency becomes very evident at 500 K where there is a wide size range $60 < N < 70$ in which the structures are fluctuating fast among different symmetries, and frequently these structures cannot be classified. There, the entropic contribution dominates. A sequence of snapshots from a simulation at 500 K is given in the third and fourth columns of Figs. 3 and 4: clear Dh structures are seen starting from $N = 69$ (second snapshot in Fig. 4), but they are still fluctuating up to $N = 71$. Above this size, the decahedral symmetry holds. Decahedra are thus found in a quite narrow size range at 500 K. Increasing further the growth temperature, the size interval of Dh structures shrinks, and at 550 K decahedra are never found around $N = 75$. At this T , the $(2, 2, 2)m$ -Dh is melted, and the minimum in $\bar{\Delta}(N)$ at $N = 75$ has disappeared (see Fig. 2). Well ordered structures are found only in a narrow range around $N = 55$, and they are classified as icosahedra. At $N \geq 58$ we recover only melted structures, and the CNA percentages stay practically constant. At 600 K also the 55 Ih is melted, so that melted structures are found in the whole size range, and no minima are found in $\bar{\Delta}(N)$.

We may compare our results with the minimum-energy growth sequence in Ref. [7]. There, Ag was modeled by Sutton-Chen potentials; Ih structures were obtained for $55 \leq N \leq 62$ and Dh ones at $63 \leq N \leq 75$, with the exception of $N = 68$, where a close packed structure, with stacking sequences and twin planes, was found. In our simulations we were able to find growth sequences (in the intermediate T range, where kinetic trapping is not important and where the entropic contribution to the free energy is not yet dominant) which are qualitatively in good agreement with the minimum-energy sequence in [7], even if we find that the transition from Ih to Dh structures is displaced to somewhat larger sizes ($N = 65$ instead of $N = 63$); more, we find decahedra at $N = 68$.

4 Conclusions

In conclusion, we have studied the growth of Ag clusters in the size range up to sizes of the order of $N = 100$ atoms, focusing on the interval $55 \leq N \leq 75$. At these sizes, Ag clusters growth takes place through sequences of non-crystalline structures, such as icosahedra and decahedra. By fixing the flux and considering different temperatures, we have found qualitatively different growth sequences. Even at very low temperatures ($T = 200$ K), in our simulations we are able to reproduce a perfect Ih at $N = 55$. Keeping on depositing atoms on this cluster at 200 K, the growth is kinetically trapped in metastable icosahedral structures up to $N = 75$, where one would expect to find an m -Dh on the basis of energetic considerations. Indeed,

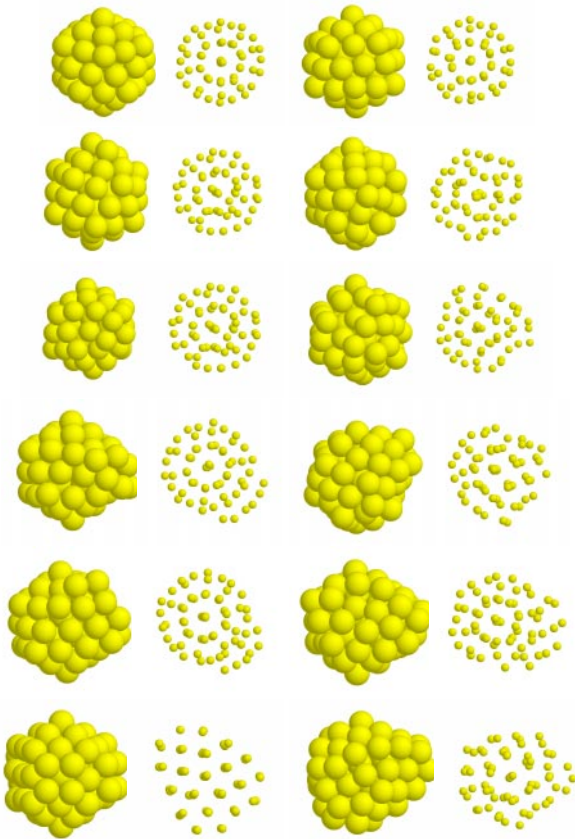


Fig. 3. Snapshots from simulations representing typical growth sequences at different temperatures. First and second columns are related to a simulation at $T = 350$ K. Third and fourth columns are related to a simulation at $T = 500$ K. For both simulations, the snapshots are taken at $N = 55, 57, 59, 61, 63, 65$ atoms from top to bottom, and each snapshot is given both in side view (first and third columns) and in top view (second and fourth columns). The side views are given in spacefill representation which is suited to show the cluster surface, while the top views are shown in a representation which is suited for looking at the inner arrangement of the cluster atoms. Both simulations start from Ih structures at $N = 55$; at $T = 350$ K the transition to Dh structures is accomplished already at $N = 65$.

the latter m -Dh is found by growing at higher T , for example in the range $300 \leq T \leq 500$ K. At 300 K kinetic trapping effects are still present: hybrid structures are formed in an intermediate size range. Between 350 and 450 K, kinetic trapping is no more important, and the transition is quite sharp at $N = 65$ – 67 . At higher T , entropic effects become evident, and the transition is smeared out again, with an interval of fluctuating structures in between 60 and 70 atoms (see the results at 500 K). Finally, at 550 K the 75 Dh is melted, and at 600 K also the 55 Ih is melted.

F. Baletto and R. Ferrando acknowledge support from the Italian MURST under the project N. 9902112831. The CRMC2 is associate to the Universities of Aix-Marseille II and III.

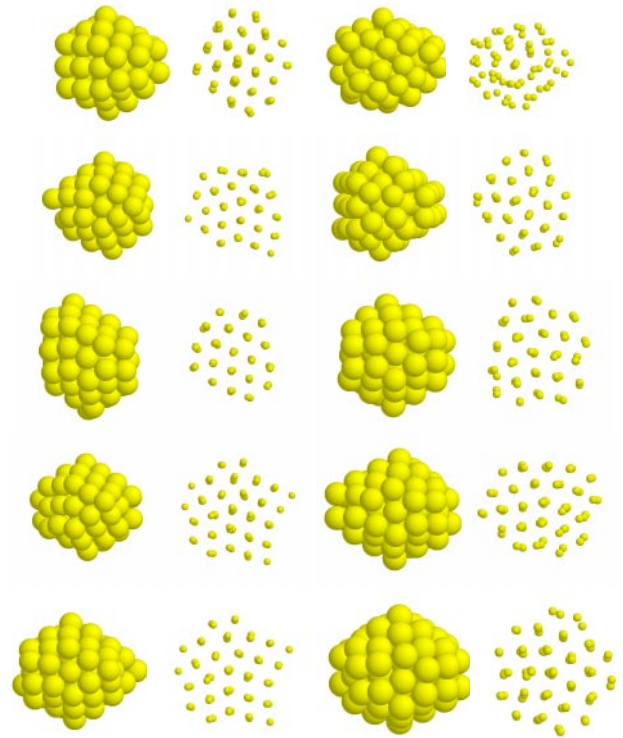


Fig. 4. The same simulations as in Fig. 3, but the snapshots are taken at $N = 67, 69, 70, 71, 73, 75$. At 500 K the transformation to Dh begins above $N = 67$ and is completed at $N \geq 71$. At $N = 69$ structures are fluctuating.

References

1. C.R. Henry, Surf. Sci. Rep. **31**, 231 (1998).
2. P. Jensen, Rev. Mod. Phys. **71**, 1695 (1999).
3. W. Harbich, in *Metal Clusters at Surfaces*, Springer Series in Clusters Physics (Springer, Berlin, 2000), Chap. 4.
4. C.L. Cleveland, U. Landman, J. Chem. Phys. **94**, 7376 (1991).
5. V.B. Koutecký, L. Cespiva, P. Fantucci, J. Koutecký, J. Chem. Phys. **98**, 7981 (1993).
6. C. Mottet, G. Tréglia, B. Legrand, Surf. Sci. **383**, L719 (1997).
7. J.P.K. Doye, D.J. Wales, New J. Chem. **22**, 733 (1998).
8. K. Michaelian, N. Rendón, I.L. Garzon, Phys. Rev. B **60**, 2000 (1999).
9. F. Baletto, C. Mottet, R. Ferrando, Phys. Rev. Lett. **84**, 5544 (2000).
10. T.P. Martin, Phys. Rep. **273**, 199 (1996).
11. L.D. Marks, Rep. Prog. Phys. **57**, 603 (1994).
12. D. Reinhard, B.D. Hall, D. Ugarte, R. Monot, Phys. Rev. B **55**, 7868 (1997).
13. S. Valkealahti, M. Manninen, Phys. Rev. B **57**, 15533 (1998).
14. F. Baletto, C. Mottet, R. Ferrando, Surf. Sci. **446**, 31 (2000).
15. M. Guillopé, B. Legrand, Surf. Sci. **215**, 577 (1989).
16. D. Faken, H. Jónsson, Comp. Mat. Sci. **2**, 279 (1994).